Published in final edited form as:
Circulation. 2012 June 12; 125(23): 2844–2853. doi:10.1161/CIRCULATIONAHA.111.060889.

Ventricular Assist Device Implantation Corrects Myocardial Lipotoxicity, Reverses Insulin Resistance and Normalizes Cardiac Metabolism in Patients with Advanced Heart Failure

Aalap Chokshi, MD[1], **Konstantinos Drosatos, PhD**[2], **Faisal H. Cheema, MD**[3], **Ruiping Ji, MD**[1], **Tuba Khawaja, MD**[1], **Shuiqing Yu, BS**[1], **Tomoko Kato, MD**[1], **Raffay Khan, MD**[2], **Hiroo Takayama, MD**[3], **Ralph Knöll, MD, PhD**[4], **Hendrik Milting, PhD**[5], **Christine S. Chung, MD**[1], **Ulrich Jorde, MD**[1], **Yoshifumi Naka, MD, PhD**[3], **Donna M. Mancini, MD**[1], **Ira J. Goldberg, MD**[2], and **P. Christian Schulze, MD, PhD**[1]

[1]Division of Cardiology, Dept of Medicine, Columbia University Medical Center, New York, NY

[2]Division of Preventive Medicine & Nutrition, Dept of Medicine, Columbia University Medical Center, New York, NY

[3]Division of Cardiothoracic Surgery, Dept of Surgery, Columbia University Medical Center, New York, NY

[4]Imperial College, London, United Kingdom

[5]Herzzentrum Bad Oeynhausen, Bad Oeynhausen, Germany

Abstract

Background—Heart failure is associated with impaired myocardial metabolism with a shift from fatty acids to glucose utilization for ATP generation. We hypothesized that cardiac accumulation of toxic lipid intermediates inhibits insulin signaling in advanced heart failure and that mechanical unloading of the failing myocardium corrects impaired cardiac metabolism.

Methods and Results—We analyzed myocardium and serum of 61 patients with heart failure (BMI 26.5±5.1 kg/m^2, age 51±12 years) obtained during left ventricular assist device (LVAD) implantation and at explantation (mean duration 185±156 days) and from 9 controls. Systemic insulin resistance in heart failure was accompanied by decreased myocardial triglyceride and overall fatty acid content but increased toxic lipid intermediates, diacylglycerol and ceramide. Increased membrane localization of protein kinase C isoforms, inhibitors of insulin signaling, and decreased activity of insulin signaling molecules Akt and FOXO, were detectable in heart failure compared to controls. LVAD implantation improved whole body insulin resistance (HOMA-IR: 4.5±0.6 to 3.2±0.5; $p<0.05$) and decreased myocardial levels of diacylglycerol and ceramide while triglyceride and fatty acid content remained unchanged. Improved activation of the insulin/PI3kinase/Akt signaling cascade after LVAD implantation was confirmed by increased phosphorylation of Akt and FOXO, which was accompanied by decreased membrane localization of protein kinase C isoforms after LVAD implantation.

Correspondence: P. Christian Schulze, MD, PhD, Columbia University Medical Center, Center for Advanced Cardiac Care, Department of Medicine, Division of Cardiology, 622 West 168th Street, PH 10, Room 203, New York, NY 10032, Tel: 212-305-6916, Fax: 212-342-5355, pcs2121@mail.cumc.columbia.edu.

Conflict of Interest Disclosures: None

Conclusions—Mechanical unloading after LVAD implantation corrects systemic and local metabolic derangements in advanced heart failure leading to reduced myocardial levels of toxic lipid intermediates and improved cardiac insulin signaling.

Keywords

heart failure; lipid toxicity; metabolism; myocardial metabolism; ventricular assist device

Advanced heart failure (HF) is associated with structural, functional, inflammatory and metabolic derangements of the failing myocardium that develop and worsen during progression of the disease state.[1, 2] Metabolic abnormalities of the failing myocardium are characterized by transcriptional changes with suppression of genes regulating fatty acid uptake and oxidation while the expression of genes controlling glucose metabolism remain relatively stable, [2–4] a transcriptional program that is typical of embryogenesis.[1, 5, 6] The overall net result is a relative decrease in the metabolism and oxidation of fatty acids (FAs) and a shift towards glucose for primary ATP generation. These changes are also accompanied by profound mitochondrial dysfunction and impaired overall oxidative metabolism.[7]

Besides this myocardial dysbalance of glucose and FA metabolism, patients with advanced HF also develop systemic insulin resistance (IR) and worse IR correlates with greater morbidity and mortality.[8] Circulating proinflammatory cytokines such as TNFα and IL1β as well as dysregulation of adipokines have been linked to the development and progression of IR in HF,[9] which parallels metabolic derangements previously described in patients with abnormal glucose homeostasis indicative of early diabetes mellitus.[10]

The complex network of cellular lipid metabolism pathways must supply substrates for generation of ATP via mitochondrial beta-oxidation, production of cellular structural components and creation of signaling molecules that regulate a number of cellular processes including insulin signaling.[11] Less than 5% of total body triglycerides are stored in the non-adipose tissues such as skeletal muscle and myocardium; nevertheless, these neutral lipids can serve as an important energy storage form while pathologic lipid accumulation in skeletal muscle can trigger insulin resistance.[12] Several intermediates of lipid metabolism have toxic pro-apoptotic and pro-inflammatory actions.[13–15] Skeletal muscle and myocardium of patients with diabetes mellitus have increased levels of diacylglycerol (DAG) and ceramide, which have been directly linked to mitochondrial dysfunction and impaired intracellular glucose and FA oxidation.[14, 16] Intracellular lipid accumulation associated with such deleterious effects on cellular function has been termed “lipotoxicity”. Proof that lipids themselves are toxic has come from studies showing that overexpression of enzymes that increase intracellular lipid levels leads to insulin resistance, and gene deletion of these enzymes, which reduces toxic levels of intracellular lipids, improves insulin sensitivity.[13, 17–20] In addition, induced lipid accumulation in the heart leads to cardiac dysfunction.[13, 15, 21]

The aim of our study was to compare levels of intracellular lipids between patients with advanced HF and controls and to test the hypothesis that mechanical unloading through left ventricular assist device (LVAD) implantation leads to reversal of metabolic derangements in the failing myocardium.

Methods

Patient Cohort and Sample Collection

We retrospectively analyzed 61 patients (52 male, 9 female) with advanced HF undergoing LVAD implantation at Columbia University Medical Center. Patients received either pulsatile-flow LVADs (n=30) or continuous-flow LVADs (n=31). Clinical and laboratory characteristics of all patients and hemodynamic conditions within 5 days before LVAD implantation and explantation were collected.

Myocardial specimens were collected from a subset of patients (n=21) and blood samples were obtained from all patients (n=61) at the time of LVAD implantation for end stage HF as a bridge-to-transplantation and at the time of LVAD explantation during cardiac transplantation. Control blood samples were obtained from patients without cardiovascular disease recruited at Columbia University Medical Center (n=10). Control myocardial samples (n=6) were obtained from a tissue bank of de-identified specimens collected from non-failing hearts determined to be unusable for cardiac transplantation due to acute recipient issues or donor coronary artery disease, but without evidence of previous infarction. The newly obtained heart samples were immediately snap frozen, placed in liquid nitrogen for transport and stored at −80C until final analysis.

The present study was approved by the Institutional Review Board of Columbia University. All patients provided written informed consent before inclusion into the study.

Echocardiographic Analysis

Conventional echocardiograms were obtained from all patients within 5 days before LVAD implantation and at 1 month after the surgery (Sonos-5500® or Sonos-7500®; Philips Healthcare Corp, Andover, MA, USA). The routine standard echocardiographic examination included M-mode, 2D-echocardiogram and Doppler study for measurements of ventricular septal and posterior wall thickness, end-systolic and end-diastolic LV diameters (LVESD and LVEDD). The LV ejection fraction (LVEF) was calculated by biplane Simpson's method from apical 4- and 2-chamber views. Mitral inflow was obtained by pulsed-wave Doppler echocardiography with the sample volume between mitral leaflet tips during diastole, and peak early (E) and late (A) transmitral filling velocities and their ratio (E/A), and deceleration time of E were measured. The peak positive dP/dt (dP/dt_{max}, first derivative of LV pressure with respect to time) as an index of contractility was calculated based on continuous wave Doppler determination of the velocities in mitral regurgitant jets.[19] Early diastolic annular velocity (E') was obtained by placing a tissue Doppler sample volume at the septal and lateral mitral annulus in the apical 4 chamber view and the E/E' ratio was calculated. Measurements were performed from 5 cardiac cycles and averaged.

Serum Analysis

Venous blood samples were collected and stored after centrifugation at −70°C until the assays were performed. Levels of insulin were measured with commercially available enzyme-linked immunosorbent assay (ELISA) kits (CalBiotech, Austin Drive Spring Valley, CA). The Homeostatic Model of Analysis - Insulin resistance (HOMA-IR) was utilized to described levels of insulin resistance in all patients and controls.[22] Circulating levels of BNP were analyzed by the institutional core laboratory.

Tissue Culture

A human ventricular cardiomyocyte-derived cell line, designated AC-16, was kindly provided by M. M. Davidson.[23] Cells were maintained in Dulbecco's Modified Eagle Medium:Nutrient Mixture F-12 (Ham) (DMEM:F12) (Invitrogen, Carlsbad CA).

Experiments were performed on cells at 70–80% confluence after four hours of starvation. Cells were exposed to 0.4 mM palmitic acid (PA) (Sigma Aldrich) in methanol conjugated with 1% FA-free bovine serum albumin (BSA) overnight (16 hours). Control cells were incubated in the presence of 0.25% vehicle (methanol). After overnight treatment with palmitic acid (0.4 mM for 16 hours), cells were incubated for different time intervals with 500 nm insulin (Sigma Aldrich) diluted in HEPES buffer for different time intervals in the presence or absence of PKC inhibitor (RO-318220, Sigma, USA).

Gene Expression Analysis

Total RNA was extracted using standard methods and the abundance of specific mRNAs was determined by RT-PCR with a Prism 7700 Sequence Detector (Perkin-Elmer, Foster City, CA, USA). Sequences of primers and TaqMan probes specific for CD36, CPT1, ACO, GLUT1, GLUT4, IR, PDK4, ATGL, HSL, DGAT1 and DGAT2, and BNP were described previously.[6, 13, 15, 18] Gene expression was normalized using expression of 18S mRNA and expressed as relative expression.

Protein Analysis

Tissues and cells were lysed in 200μl of lysis buffer containing 20mM Tris-HCl (pH 8.0), 2mM EDTA, 2mM EGTA, 6mM β-mercaptoethanol, 0.1mM sodium vanadate, 50mM sodium fluoride, protease inhibitors and phosphatase inhibitors (Roche, Indianapolis, IN). Protein extraction was performed using standard techniques. Protein lysates from cells were resolved on 4–15 % SDS PAGE reducing gels (Bio-Rad), transferred to PVDF membranes (Bio-Rad), blocked in 5% milk/TRIS-buffered saline, and probed with antibodies for detection of phosphoAkt, total Akt, phosphoFoxo, total Foxo and GAPDH (all from Cell Signaling Technologies Inc, MA, USA). Membranes were washed, incubated with appropriate secondary antibodies conjugated to horseradish peroxidase, washed in TBS-T and detected by using ECL Western Blotting System Kit (Thermo Scientific).

Analysis of PKC isoform localization and activity was performed after protein isolation. Membrane and cytosolic fractions were separated by ultracentrifugation at 33,000 rpm for 1h. 25 μg from each fraction was applied to SDS-PAGE and transferred onto nitrocellulose membranes and PKC isoforms detected using specific antibodies (PKCα from Millipore, Billerica, MA; PKCβ, PKCδ and PKCε from Santa Cruz Biotechnology, Santa Cruz, CA). Specific PKC activity was measured using the non-radioactive PKC kinase activity kit (Assay Designs, Ann Arbor, MI) as previously described.[15]

Lipid Measurements

Total lipids were extracted by the Folch method of extraction. Briefly, 25–50 mg of tissue or cell pellet were homogenized in PBS and chloroform:methanol (2:1). The organic phase was separated twice and dried. The dried lipids were solubilized in 1% Triton X-100, dried, and resuspended in distilled water. Cardiac triglyceride content was measured using the Infinity Triglycerides kit (Thermo Scientific) with the Matrix Plus Chemistry Reference Kit (Verichem Laboratory Inc.) as standard. Total FAs were quantified as sum of individual FAs detected by liquid chromatography-mass spectrometry (LC/MS)-based lipidomics (Waters Xevo TQ MS ACQUITY UPLC system, Waters, Milford, MA). Total DAG and ceramide were detected using the diacylglycerol kinase method as previously described.[24]

Histology

Histopathology was assessed on myocardial specimens obtained at the time of LVAD implantation and at the time of explantation after paraffin fixation and H&E and Masson's trichrome staining. Myocardial fibrosis was quantified on serial sections using Masson's

trichrome staining for the detection of collagen. Area of fibrosis was analyzed using the ImagePro software (NIH) and expressed as percent of total section area. Myocyte cross-sectional area (CSA) was analyzed after semiquantitative analysis with circumferential markings of the myocytes using ImagePro software and expression of average cross-sectional area and distribution of fiber sizes within each sample.

Statistical Analysis

Data are presented as means ± SD. Normality was evaluated for each variable from normal distribution plots and histograms and by the Kolmogorov-Smirnov test. The echocardiographic and laboratory variables, as well as serum and myocardial gene expression of before and after surgery, and the % changes of the variables through the surgery were compared between the groups with Student's unpaired two-tailed *t*-test for groups with parametric distribution and the Mann-Whitney-U test for samples with non-parametric distribution. The values before and after the surgery in each group of patients were assessed with Student's paired t test for groups with parametric distribution and the Wilcoxon test for samples with non-parametric distribution. Comparisons of more than two groups were performed using ANOVA with appropriate post-hoc testing. A p value of <0.05 was considered statistically significant. All data were analyzed using the SPSS version 18 (IBM, USA).

Results

Baseline Characteristics

We analyzed a total of 61 patients undergoing placement of a LVAD at our institution between 1998 and 2010. Clinical characteristics of all patients are summarized in Table 1. The duration of LVAD support ranged from 31 to 662 days (mean 176 days). Patients with HF had generalized insulin resistance by HOMA-IR (3.7±1.8 in HF vs. 1.1±0.6 in controls; $p<0.01$).

Echocardiographic Assessment

Echocardiographic parameters before and after LVAD placement are listed in Table 2. In short, LVEDD and LVESD after LVAD implantation was significantly smaller compared to the parameters before the surgery in both groups. LVEF increased during mechanical support. Additional parameters are listed in Table 2.

Impaired Insulin Signaling in the Failing Human Myocardium

Next, we analyzed activation of the insulin signaling cascade and downstream targets of the insulin receptor namely the IRS/Akt/Foxo signaling cascade in myocardial samples collected during LVAD implantation and explantation as well as in control samples. Samples of failing human myocardium revealed impaired phosphorylation of Akt and Foxo compared to control samples indicating a reduced myocardial activation of the insulin signaling cascade in advanced human HF consistent with cardiac insulin resistance (Figure 1).

Increased Levels of DAG and Ceramide in the Failing Human Myocardium

We further determined levels of intracellular lipids in failing human myocardium for comparison with non-failing cardiac samples. Significantly decreased levels of triglycerides and free FAs were noted in failing human myocardium compared to control samples. In contrast, a strong increase in intracellular levels of the toxic lipid intermediates DAG and ceramide were found in samples from patients with advanced HF compared to control samples (Figure 2A). These findings demonstrate myocardial accumulation of toxic lipid

intermediates in patients with advanced HF while neutral lipids and free FAs remained decreased.

Reduction of FFA and TG with accumulation of DAG and ceramide was accompanied by significant reduction in gene expression of CD36 and CPT1, markers of FA uptake and oxidation, as well as GLUT4, marker of glucose uptake. PDK4 was suppressed indicating increased glucose oxidation consistent with previous findings of abnormal metabolic gene regulation in severe HF. Impaired mitochondrial oxidative metabolism was further indicated by reduced expression levels of PGC1α. Of note, expression of DGAT1, the rate limiting enzyme catalyzing the conversion of DAG to monoacylglycerol as well as ATGL, which catalyzes triglyceride to DAG degradation, was decreased in advanced HF compared to controls (Figure 2B).

Lipid Overload Inhibits Cardiomyocyte Insulin Signaling Through PKC Activation

We next analyzed the impact of lipid overload on insulin signaling in cardiomyocytes *in vitro*. AC16 cells, a human cardiomyocyte cell line,[23] was utilized for the analysis of the insulin signaling cascade. First, we confirmed that overnight incubation with PA increased overall intracellular lipid content using oil-red-O staining. Further, we quantified the cellular content of triglyceride, DAG and ceramide; they all showed a significant increase after overnight stimulation with PA (Figure 3A). We then tested whether PA affects insulin signaling through the PI3K/Akt signaling cascade. Insulin stimulation of AC16 cells resulted in a strong activation of Akt that was inhibited by overnight incubation with PA indicating that PA incubation and the associated increase in intracellular lipids blocks insulin-induced phosphorylation of Akt. Next, we tested the impact of PA stimulation on PKC activity in AC16 cells. Incubation of AC16 cells with PA stimulated total PKC activity (+51%; $p<0.05$ vs. unstimulated cells) (Figure 3C). Finally, inhibition of insulin-mediated Akt phosphorylation in cells pre-incubated with PA was reduced in the presence of a PKC inhibitor. These findings indicate that PKC is necessary for inhibition of Akt phosphorylation in cardiomyocytes in the setting of high intracellular lipid levels (Figure 3D).

Mechanical Unloading of the Failing Myocardium Improves Systemic Insulin Resistance and Enhances Cardiac Insulin Signaling

LVAD implantation reduced fibrotic tissue accumulation (31.7±2.7 to 22.7±5.9%, $p=0.016$) and myocyte CSA (221.5±9.1 vs. 124.6±35.0 μm^2, $p<0.0001$) indicating mechanical unloading of the failing myocardium.

HF patients following LVAD implantation showed reduced fasting glucose and HbA1c levels (Table 3). This was accompanied by a reduction in circulating levels of insulin. These changes resulted in a significant decrease in calculated HOMA-IR, consistent with improved systemic insulin sensitivity, in patients with advanced HF following LVAD placement (3.7±1.8 in HF vs. 2.5±0.8 post-LVAD; $p<0.05$) (Figure 4 and Supplemental Figure 1).

Analysis of insulin signaling in myocardial samples obtained from patients before and after VAD implantation showed a dramatic increase in phosphorylation levels of Akt and Foxo (Figure 5). These findings indicate enhanced myocardial insulin signaling in response to mechanical unloading of the failing myocardium.

Reduced Myocardial Toxic Lipids after Mechanical Unloading

We next analyzed levels of intracellular lipids and FAs in myocardial samples obtained from patients before and after LVAD implantation. No changes were detectable in the triglyceride or FA content in response to LVAD implantation (p=NS). In contrast, levels of DAG and

ceramide were reduced following LVAD placement (DAG: −31%; p<0.05 vs. pre-LVAD; ceramide: −53%; p<0.05 vs. pre-LVAD) (Figure 6A). Surprisingly, these changes were accompanied by increased expression of CD36 indicating higher FA uptake. This appeared to be compensated by greater FA oxidation as both and CPT1 and PDK4 mRNA levels increased following LVAD implantation (Figure 6B). Greater oxidation of incoming lipids might prevent their conversion to cellular toxic lipids with LVAD placement as DGAT 1 and 2 mRNA expression did not change following mechanical unloading. In line with previous reports on impaired mitochondrial function in advanced HF and the corrective impact of mechanical unloading,[25] expression of PGC1α, a central regulator of oxidative metabolism, also increased following LVAD implantation (+145%; p<0.05 vs. pre-LVAD) consistent with an overall improvement of mitochondrial function and oxidative metabolism (Figure 6B). Further, activation of AMPK also increased in the myocardium following LVAD implantation compared to advanced HF (+223%; p<0.05 vs. pre-LVAD) (Figure 6C).

Reduced PKC Activity in Response to VAD implantation

Finally, we analyzed levels of cytoplasmic and membrane-bound PKC isoforms to determine the activation. There was a clear reduction in membrane associated PKCα, indicative of a reduced PKCα activation in the myocardium of patients following LVAD implantation (−34%; p<0.05 vs. pre-LVAD). PKCδ showed a non- statistical significance trend towards reduced activation (−27%, p=0.08 vs. pre-LVAD). No differences were noted in PKCθ activity levels in response to LVAD implantation. These data indicate reduced activation of PKC following mechanical unloading of the failing myocardium (Figure 7).

Discussion

Although it is well known that HF alters glucose and lipid metabolism, our current study demonstrates for the first time that patients with advanced HF have a novel metabolic cardiac phenotype indicative of myocardial lipotoxicity accompanied by insulin resistance in non-obese patients. A central part of this phenotype is reduced insulin signaling, PKC activation and accumulation of DAG and ceramide. Mechanical unloading corrects each of these abnormalities (Figure 8).

Advanced HF leads to an imbalance of catabolic and anabolic pathways favoring catabolism and loss of muscle mass in advanced stages of the disease.[26] In part, this might result from insulin resistance, which has been characterized as a prognostic factor defining poor outcome.[8, 27] Impaired glucose homeostasis in HF has been linked to increased catecholamine levels,[28] low grade inflammation,[8] reduced blood flow and potentially immobilization. The use of LVADs in our patients corrected many of these abnormalities and improved HOMA-IR. In the absence of HF, metabolic changes associated with insulin resistance are most commonly referred to as the “metabolic syndrome” with obesity being the most prevalent. Metabolic risk factors established in individuals without overt disease such as lipid abnormalities and obesity do not carry the same risk in patients with advanced HF; in fact, some metabolic abnormalities (e.g. high cholesterol levels or increased BMI) carry a survival benefit in this patient population.[29, 30] This apparent paradox has been characterized as the “lipid paradox” or “obesity paradox” in patients with HF.

One characteristic of the metabolic syndrome and diabetes is accumulation of signaling lipids; these lipids are thought to cause insulin resistance and other types of cellular dysfunction. Lipotoxicity is a consequence of either increased lipid – especially FA - uptake or impaired lipid oxidation and storage leading to accumulation of DAG and/or ceramide. Both, DAG and ceramide have been implicated in insulin resistance,[14] mitochondrial dysfunction,[14, 31] and apoptosis.[32] Genetic alterations in mice that increase tissue DAG lead

to insulin resistance,[14] while prevention of ceramide synthesis negates saturated fat-induced insulin resistance.[33] Analysis in hearts from patients with severe HF show a marked suppression of genes associated with both FA oxidation and non-toxic storage of lipid in triglyceride. Although CD36, a well-established mediator of cardiac FA uptake was reduced, it is likely that residual FAs entering the heart are re-routed into synthesis of DAG and ceramide leading to accumulation of these signaling lipids.

Lipid accumulation can be a cause as well as a consequence of HF. A series of genetically altered mice have been created that have lipid accumulation due to excess FA uptake or a reduction in oxidation. These include overexpression of genes that cause greater trapping of FAs,[34, 35] reduced activation of PPARs (PPARD ko and ATGL ko),[36, 37] and, paradoxically, PPARα and PPARγ,[20, 21, 38] which must cause greater lipid uptake than oxidation. Several of these models have activation of PKC and development of hypertrophy.[21] Therefore, lipid accumulation aside from altering metabolism might exacerbate HF.

Increased intracellular lipid accumulation in HF has been described in previous studies and was linked to obesity and diabetes mellitus. One prior human study showed increased levels of triglycerides in the myocardium of obese (BMI>30 kg/m^2) and diabetic patients with advanced HF undergoing heart transplantation.[39] These findings are well in line with animal studies showing increased myocardial levels of triglycerides in murine models of diabetes.[21, 38, 40] In contrast, animal models of HF secondary to transaortic banding under non-diabetic conditions are associated with reduced myocardial triglyceride content.[41, 42] Unlike in our current study, previous human studies have not differentiated between lipid subspecies. Limited data are available to ascertain whether a non-diabetic group with advanced HF also has an increase in various cardiac lipids. Our current study found no increase in FAs or triglycerides while ceramide and DAG levels increased in the non-obese patient cohort. Perhaps this was due to a limited number of patients with diabetes and obesity; the average BMI of our patients was 26.5 kg/m^2. We also found a uniform decrease in gene expression of regulators of primarily lipid metabolism and oxidation. In particular, levels of DGAT1 and ATGL were reduced. We believe that the decreased levels of triglycerides and FAs represent a depletion of energy storage pools in the failing myocardium and the diversion of incoming FAs into DAG and ceramide. The underlying pathophysiologic mechanism is likely a failure to oxidize FAs due to mitochondrial dysfunction, a phenomenon which has been well described in advanced HF. Alternatively, impaired myocardial lipolysis might be a primary mechanism leading to reduced FA oxidation. Our patients showed reduced ATGL expression and ATGL deficiency in mice leads to decreased PPARα activation and defective lipid use.

One of the central findings of this study is the beneficial effect of mechanical unloading on cardiac metabolism in the failing myocardium. The advent of VADs has improved the therapeutic options for patients with advanced HF and is now an established intervention in patients awaiting cardiac transplantation. We here show that improved hemodynamics after VAD implantation are accompanied by reduced whole body and cardiac insulin resistance and improved glucose homeostasis along with a reduction in levels of the toxic lipid intermediates DAG and ceramide. Activation of PKC by toxic lipid intermediates with subsequent inhibition of Akt signaling represents a direct molecular link between HF-associated lipotoxicity and myocardial insulin resistance. It remains to be clarified which molecular mechanisms connect biomechanical cardiac stress with impaired metabolism. However, the finding of reversible myocardial metabolic derangement following mechanical unloading might uncover novel therapeutic strategies for the treatment of advanced HF patients. While we found increased activation of AMPK and enhanced expression of PGC1α after VAD implantation, partially correcting the decreased activation state found in HF samples compared to controls, other mechanisms might contribute to the improvement in

metabolic state. Increased expression of PGC1α after mechanical unloading also suggests improvement in oxidative capacity and mitochondrial dysfunction of the failing myocardium.

Our study has several limitations. First, we have only incomplete clinical and laboratory data available on the control patients which is related to the use of samples from a de-identified tissue depository. Further, we could not analyze subgroups of patients such as diabetic versus non-diabetic patients, obese versus non-obese patients, ischemic versus non-ischemic cardiomyopathies due to the limited number of patients in our tissue substudy. Further, effects of aging and gender differences are unclear due to the small number of patients in our study.

In conclusion, this study represents the first analysis of cellular pathways of lipotoxicity and insulin resistance in patients with advanced HF. Our study suggests a novel pathway of lipotoxic cellular damage contributing to myocardial insulin resistance through accumulation of the toxic lipid intermediates DAG and ceramide. PKC activation may be a crucial mediator of this pathophenomenon. Further studies should focus on potential therapeutic interventions correcting impaired cardiac metabolism and insulin resistance through PKC inhibition or alterations in lipid metabolism that prevent the accumulation of toxic lipid intermediates.

Supplementary Material

Refer to Web version on PubMed Central for supplementary material.

Acknowledgments

Funding Sources: This work was supported by grants from the NHLBI (K23 HL095742-01, P30 HL101272-01, UL1 RR 024156, HL073029, and HL45095) and the Herbert and Florence Irving Scholar Award to Dr. Schulze. Dr. Khan was supported by a T32007343 from the NHLBI. Aalap Chokshi was supported by the Doris Duke Fellowship Program. Dr. Drosatos is supported by a post-doctoral fellowship award by the American Heart Association, Founders Affiliate.

References

1. Hunter JJ, Chien KR. Signaling pathways for cardiac hypertrophy and failure. N Engl J Med. 1999; 341:1276–1283. [PubMed: 10528039]
2. Neubauer S. The failing heart--an engine out of fuel. N Engl J Med. 2007; 356:1140–1151. [PubMed: 17360992]
3. Tian R. Transcriptional regulation of energy substrate metabolism in normal and hypertrophied heart. Curr Hypertens Rep. 2003; 5:454–458. [PubMed: 14594563]
4. Ingwall JS. On substrate selection for atp synthesis in the failing human myocardium. Am J Physiol Heart Circ Physiol. 2007; 293:H3225–H3226. [PubMed: 17921320]
5. Razeghi P, Young ME, Alcorn JL, Moravec CS, Frazier OH, Taegtmeyer H. Metabolic gene expression in fetal and failing human heart. Circulation. 2001; 104:2923–2931. [PubMed: 11739307]
6. Depre C, Shipley GL, Chen W, Han Q, Doenst T, Moore ML, Stepkowski S, Davies PJ, Taegtmeyer H. Unloaded heart in vivo replicates fetal gene expression of cardiac hypertrophy. Nat Med. 1998; 4:1269–1275. [PubMed: 9809550]
7. Ventura-Clapier R, Garnier A, Veksler V. Energy metabolism in heart failure. J Physiol. 2004; 555:1–13. [PubMed: 14660709]
8. Doehner W, Rauchhaus M, Ponikowski P, Godsland IF, von Haehling S, Okonko DO, Leyva F, Proudler AJ, Coats AJ, Anker SD. Impaired insulin sensitivity as an independent risk factor for mortality in patients with stable chronic heart failure. J Am Coll Cardiol. 2005; 46:1019–1026. [PubMed: 16168285]

9. McEntegart MB, Awede B, Petrie MC, Sattar N, Dunn FG, MacFarlane NG, McMurray JJ. Increase in serum adiponectin concentration in patients with heart failure and cachexia: Relationship with leptin, other cytokines, and b-type natriuretic peptide. Eur Heart J. 2007; 28:829–835. [PubMed: 17403719]
10. Saghizadeh M, Ong JM, Garvey WT, Henry RR, Kern PA. The expression of tnf-alpha by human muscle -relationship to insulin resistance. J Clin Invest. 1996; 97:1111–1116. [PubMed: 8613535]
11. Heather LC, Clarke K. Metabolism, hypoxia and the diabetic heart. J Mol Cell Cardiol. 2011; 50:598–605. [PubMed: 21262230]
12. Kim JY, van de Wall E, Laplante M, Azzara A, Trujillo ME, Hofmann SM, Schraw T, Durand JL, Li H, Li G, Jelicks LA, Mehler MF, Hui DY, Deshaies Y, Shulman GI, Schwartz GJ, Scherer PE. Obesity-associated improvements in metabolic profile through expansion of adipose tissue. J Clin Invest. 2007; 117:2621–2637. [PubMed: 17717599]
13. Park TS, Hu Y, Noh HL, Drosatos K, Okajima K, Buchanan J, Tuinei J, Homma S, Jiang XC, Abel ED, Goldberg IJ. Ceramide is a cardiotoxin in lipotoxic cardiomyopathy. J Lipid Res. 2008; 49:2101–2112. [PubMed: 18515784]
14. Yu C, Chen Y, Cline GW, Zhang D, Zong H, Wang Y, Bergeron R, Kim JK, Cushman SW, Cooney GJ, Atcheson B, White MF, Kraegen EW, Shulman GI. Mechanism by which fatty acids inhibit insulin activation of insulin receptor substrate-1 (irs-1)-associated phosphatidylinositol 3-kinase activity in muscle. J Biol Chem. 2002; 277:50230–50236. [PubMed: 12006582]
15. Drosatos K, Bharadwaj KG, Lymperopoulos A, Ikeda S, Khan R, Hu Y, Agarwal R, Yu S, Jiang H, Steinberg SF, Blaner WS, Koch WJ, Goldberg IJ. Cardiomyocyte lipids impair beta-adrenergic receptor function via pkc activation. Am J Physiol Endocrinol Metab. 2011; 300:E489–E499. [PubMed: 21139071]
16. Griffin ME, Marcucci MJ, Cline GW, Bell K, Barucci N, Lee D, Goodyear LJ, Kraegen EW, White MF, Shulman GI. Free fatty acid-induced insulin resistance is associated with activation of protein kinase c theta and alterations in the insulin signaling cascade. Diabetes. 1999; 48:1270–1274. [PubMed: 10342815]
17. Vianna CR, Huntgeburth M, Coppari R, Choi CS, Lin J, Krauss S, Barbatelli G, Tzameli I, Kim YB, Cinti S, Shulman GI, Spiegelman BM, Lowell BB. Hypomorphic mutation of pgc- 1beta causes mitochondrial dysfunction and liver insulin resistance. Cell Metab. 2006; 4:453–464. [PubMed: 17141629]
18. Choi CS, Befroy DE, Codella R, Kim S, Reznick RM, Hwang YJ, Liu ZX, Lee HY, Distefano A, Samuel VT, Zhang D, Cline GW, Handschin C, Lin J, Petersen KF, Spiegelman BM, Shulman GI. Paradoxical effects of increased expression of pgc-1alpha on muscle mitochondrial function and insulin-stimulated muscle glucose metabolism. Proc Natl Acad Sci U S A. 2008; 105:19926–19931. [PubMed: 19066218]
19. Choi CS, Savage DB, Abu-Elheiga L, Liu ZX, Kim S, Kulkarni A, Distefano A, Hwang YJ, Reznick RM, Codella R, Zhang D, Cline GW, Wakil SJ, Shulman GI. Continuous fat oxidation in acetyl-coa carboxylase 2 knockout mice increases total energy expenditure, reduces fat mass, and improves insulin sensitivity. Proc Natl Acad Sci U S A. 2007; 104:16480–16485. [PubMed: 17923673]
20. Son NH, Yu S, Tuinei J, Arai K, Hamai H, Homma S, Shulman GI, Abel ED, Goldberg IJ. Ppargamma-induced cardiolipotoxicity in mice is ameliorated by pparalpha deficiency despite increases in fatty acid oxidation. J Clin Invest. 2010; 120:3443–3454. [PubMed: 20852389]
21. Son NH, Park TS, Yamashita H, Yokoyama M, Huggins LA, Okajima K, Homma S, Szabolcs MJ, Huang LS, Goldberg IJ. Cardiomyocyte expression of ppargamma leads to cardiac dysfunction in mice. J Clin Invest. 2007; 117:2791–2801. [PubMed: 17823655]
22. Matthews DR, Hosker JP, Rudenski AS, Naylor BA, Treacher DF, Turner RC. Homeostasis model assessment: Insulin resistance and beta-cell function from fasting plasma glucose and insulin concentrations in man. Diabetologia. 1985; 28:412–419. [PubMed: 3899825]
23. Davidson MM, Nesti C, Palenzuela L, Walker WF, Hernandez E, Protas L, Hirano M, Isaac ND. Novel cell lines derived from adult human ventricular cardiomyocytes. J Mol Cell Cardiol. 2005; 39:133–147. [PubMed: 15913645]
24. Bielawska A, Perry DK, Hannun YA. Determination of ceramides and diglycerides by the diglyceride kinase assay. Anal Biochem. 2001; 298:141–150. [PubMed: 11757501]

25. Lee SH, Doliba N, Osbakken M, Oz M, Mancini D. Improvement of myocardial mitochondrial function after hemodynamic support with left ventricular assist devices in patients with heart failure. J Thorac Cardiovasc Surg. 1998; 116:344–349. [PubMed: 9699589]

26. Anker SD, Chua TP, Ponikowski P, Harrington D, Swan JW, Kox WJ, Poole-Wilson PA, Coats AJ. Hormonal changes and catabolic/anabolic imbalance in chronic heart failure and their importance for cardiac cachexia. Circulation. 1997; 96:526–534. [PubMed: 9244221]

27. Swan JW, Anker SD, Walton C, Godsland IF, Clark AL, Leyva F, Stevenson JC, Coats AJS. Insulin resistance in chronic heart failure: Relation to severity and etiology of heart failure. J Am Coll Cardiol. 1997; 30:527–532. [PubMed: 9247528]

28. Doehner W, Pflaum CD, Rauchhaus M, Godsland IF, Egerer K, Cicoira M, Florea VG, Sharma R, Bolger AP, Coats AJ, Anker SD, Strasburger CJ. Leptin, insulin sensitivity and growth hormone binding protein in chronic heart failure with and without cardiac cachexia. Eur J Endocrinol. 2001; 145:727–735. [PubMed: 11720897]

29. Anker SD, Ponikowski P, Varney S, Chua TP, Clark AL, Webb-Peploe KM, Harrington D, Kox WJ, Poole-Wilson PA, Coats AJ. Wasting as independent risk factor for mortality in chronic heart failure. Lancet. 1997; 349:1050–1053. [PubMed: 9107242]

30. Rauchhaus M, Coats AJ, Anker SD. The endotoxin-lipoprotein hypothesis. Lancet. 2000; 356:930–933. [PubMed: 11036910]

31. Park SY, Cho YR, Kim HJ, Hong EG, Higashimori T, Lee SJ, Goldberg IJ, Shulman GI, Najjar SM, Kim JK. Mechanism of glucose intolerance in mice with dominant negative mutation of ceacam1. Am J Physiol Endocrinol Metab. 2006; 291:E517–E524. [PubMed: 16638824]

32. Parra V, Eisner V, Chiong M, Criollo A, Moraga F, Garcia A, Hartel S, Jaimovich E, Zorzano A, Hidalgo C, Lavandero S. Changes in mitochondrial dynamics during ceramide-induced cardiomyocyte early apoptosis. Cardiovasc Res. 2008; 77:387–397. [PubMed: 18006463]

33. Holland WL, Brozinick JT, Wang LP, Hawkins ED, Sargent KM, Liu Y, Narra K, Hoehn KL, Knotts TA, Siesky A, Nelson DH, Karathanasis SK, Fontenot GK, Birnbaum MJ, Summers SA. Inhibition of ceramide synthesis ameliorates glucocorticoid-, saturated-fat-, and obesity-induced insulin resistance. Cell Metab. 2007; 5:167–179. [PubMed: 17339025]

34. Chiu HC, Kovacs A, Blanton RM, Han X, Courtois M, Weinheimer CJ, Yamada KA, Brunet S, Xu H, Nerbonne JM, Welch MJ, Fettig NM, Sharp TL, Sambandam N, Olson KM, Ory DS, Schaffer JE. Transgenic expression of fatty acid transport protein 1 in the heart causes lipotoxic cardiomyopathy. Circ Res. 2005; 96:225–233. [PubMed: 15618539]

35. Chiu HC, Kovacs A, Ford DA, Hsu FF, Garcia R, Herrero P, Saffitz JE, Schaffer JE. A novel mouse model of lipotoxic cardiomyopathy. J Clin Invest. 2001; 107:813–822. [PubMed: 11285300]

36. Wang P, Liu J, Li Y, Wu S, Luo J, Yang H, Subbiah R, Chatham J, Zhelyabovska O, Yang Q. Peroxisome proliferator-activated receptor {delta} is an essential transcriptional regulator for mitochondrial protection and biogenesis in adult heart. Circulation research. 2010; 106:911–919. [PubMed: 20075336]

37. Zimmermann R, Strauss JG, Haemmerle G, Schoiswohl G, Birner-Gruenberger R, Riederer M, Lass A, Neuberger G, Eisenhaber F, Hermetter A, Zechner R. Fat mobilization in adipose tissue is promoted by adipose triglyceride lipase. Science. 2004; 306:1383–1386. [PubMed: 15550674]

38. Finck BN, Lehman JJ, Leone TC, Welch MJ, Bennett MJ, Kovacs A, Han X, Gross RW, Kozak R, Lopaschuk GD, Kelly DP. The cardiac phenotype induced by pparalpha overexpression mimics that caused by diabetes mellitus. J Clin Invest. 2002; 109:121–130. [PubMed: 11781357]

39. Sharma S, Adrogue JV, Golfman L, Uray I, Lemm J, Youker K, Noon GP, Frazier OH, Taegtmeyer H. Intramyocardial lipid accumulation in the failing human heart resembles the lipotoxic rat heart. FASEB J. 2004; 18:1692–1700. [PubMed: 15522914]

40. Park SY, Cho YR, Finck BN, Kim HJ, Higashimori T, Hong EG, Lee MK, Danton C, Deshmukh S, Cline GW, Wu JJ, Bennett AM, Rothermel B, Kalinowski A, Russell KS, Kim YB, Kelly DP, Kim JK. Cardiac-specific overexpression of peroxisome proliferator-activated receptor-alpha causes insulin resistance in heart and liver. Diabetes. 2005; 54:2514–2524. [PubMed: 16123338]

41. Pound KM, Sorokina N, Ballal K, Berkich DA, Fasano M, Lanoue KF, Taegtmeyer H, O'Donnell JM, Lewandowski ED. Substrate-enzyme competition attenuates upregulated anaplerotic flux

through malic enzyme in hypertrophied rat heart and restores triacylglyceride content: Attenuating upregulated anaplerosis in hypertrophy. Circ Res. 2009; 104:805–812. [PubMed: 19213957]

42. O'Donnell JM, Fields AD, Sorokina N, Lewandowski ED. The absence of endogenous lipid oxidation in early stage heart failure exposes limits in lipid storage and turnover. J Mol Cell Cardiol. 2008; 44:315–322. [PubMed: 18155232]

Clinical Summary

The failing human heart develops metabolic derangements characterized by a shift from fatty acids to glucose utilization for ATP generation. These metabolic changes are accompanied by transcriptional changes typically seen during embryogenesis. The aim of our study was to investigate myocardial levels of toxic lipid intermediates in samples from patients with advanced heart failure compared to controls. Further, we analyzed whether mechanical unloading of the failing myocardium corrects impaired cardiac metabolism. For this purpose, we analyzed myocardium and serum of patients with advanced heart failure obtained during left ventricular assist device (LVAD) implantation and at explantation as well as from controls. Systemic insulin resistance in heart failure was accompanied by decreased myocardial triglyceride and overall FA content but increased toxic lipid intermediates, diacylglycerol (DAG) and ceramide. Several downstream signaling molecules known to regulate insulin signaling (Akt, Foxo and PKC) were also found to be dysregulated in the failing myocardium altogether favoring an insulin resistant state compared to controls. LVAD implantation improved insulin resistance and decreased myocardial levels of the toxic lipid intermediates DAG and ceramide while TG and FFA content remained unchanged. Therefore, abnormal myocardial metabolism, insulin resistance and lipotoxicity develop in human heart failure. Mechanical unloading through LVAD implantation corrects systemic and local metabolic derangements in advanced heart failure. This study characterizes metabolic changes in human heart failure with the development of cardiac lipotoxicity. Further, these findings suggest potential therapeutic implications of mechanical unloading of the failing myocardium for the correction of metabolic derangements in advanced human heart failure.

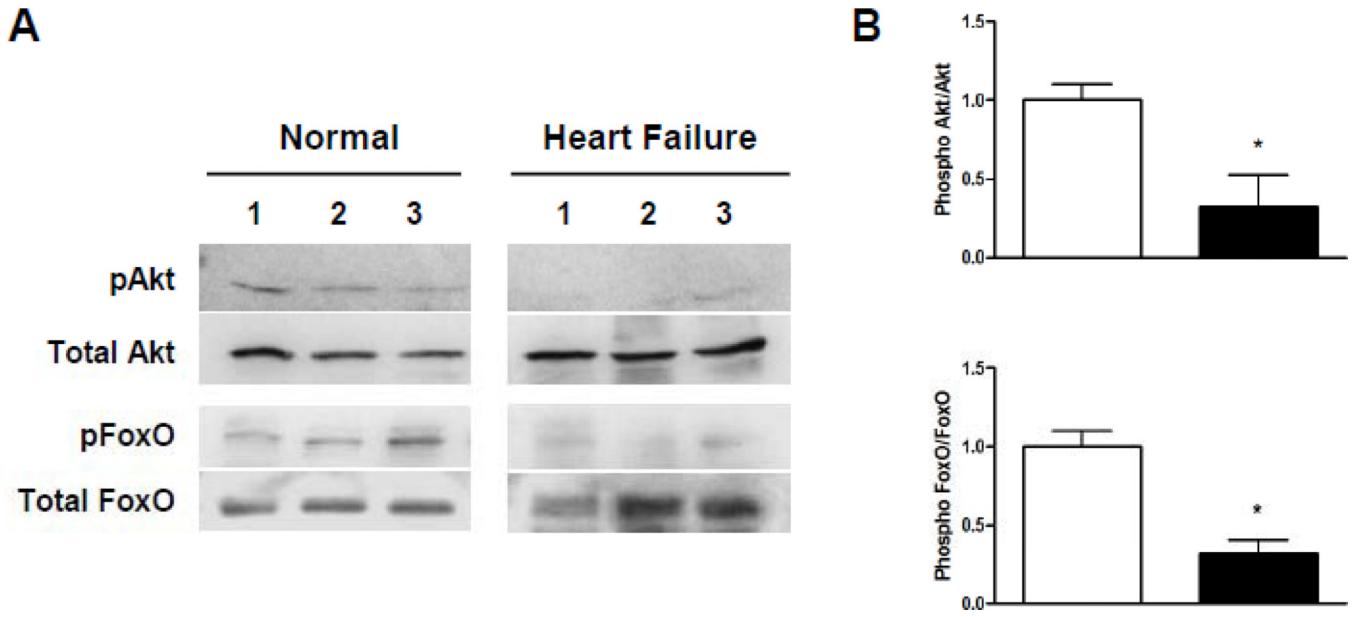

Figure 1.

Impairment of PI3Kinase/Akt signaling in human advanced HF. (**A**) Reduced activation indicated by decreased phosphorylation status of Akt and FOXO in samples from patients with advanced HF compared to control subjects (three representative samples per group). (**B**) Decreased myocardial phosphorylation levels of Akt and FOXO in patients with advanced HF compared to controls (*$p<0.05$, n=6–8 samples per group).

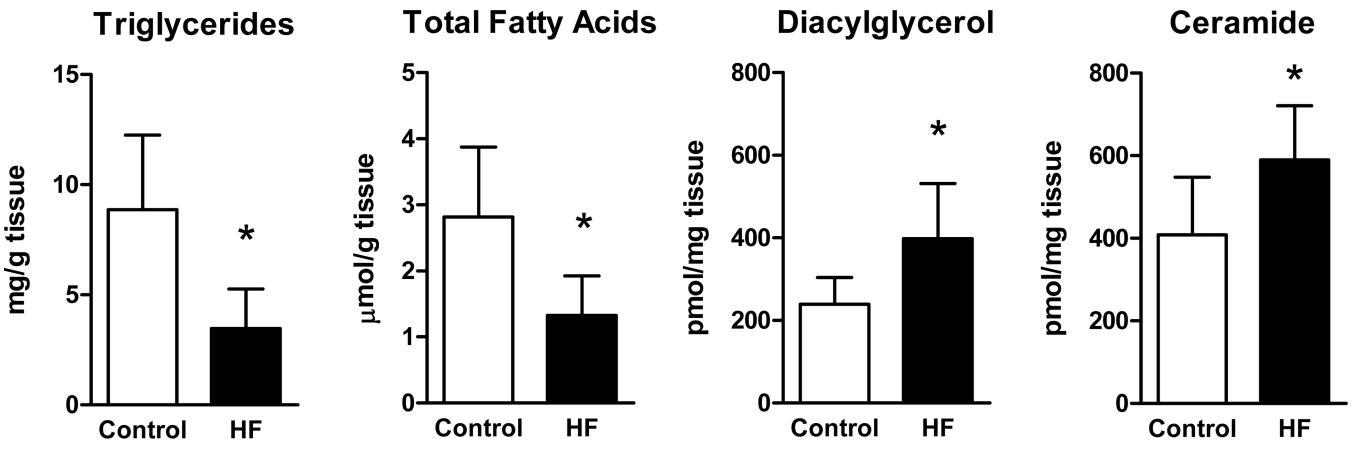

A

Figure 2.

Myocardial lipid content and transcriptional changes of glucose and lipid metabolism genes. (**A**) Myocardial lipid content in patients with advanced HF and controls. (**B**) Relative changes in gene expression of metabolic genes controlling fatty acid and glucose uptake and oxidation (empty bars – controls; filled bars – HF; n=6–8 individual patients in each group, *p<0.05 vs. controls).

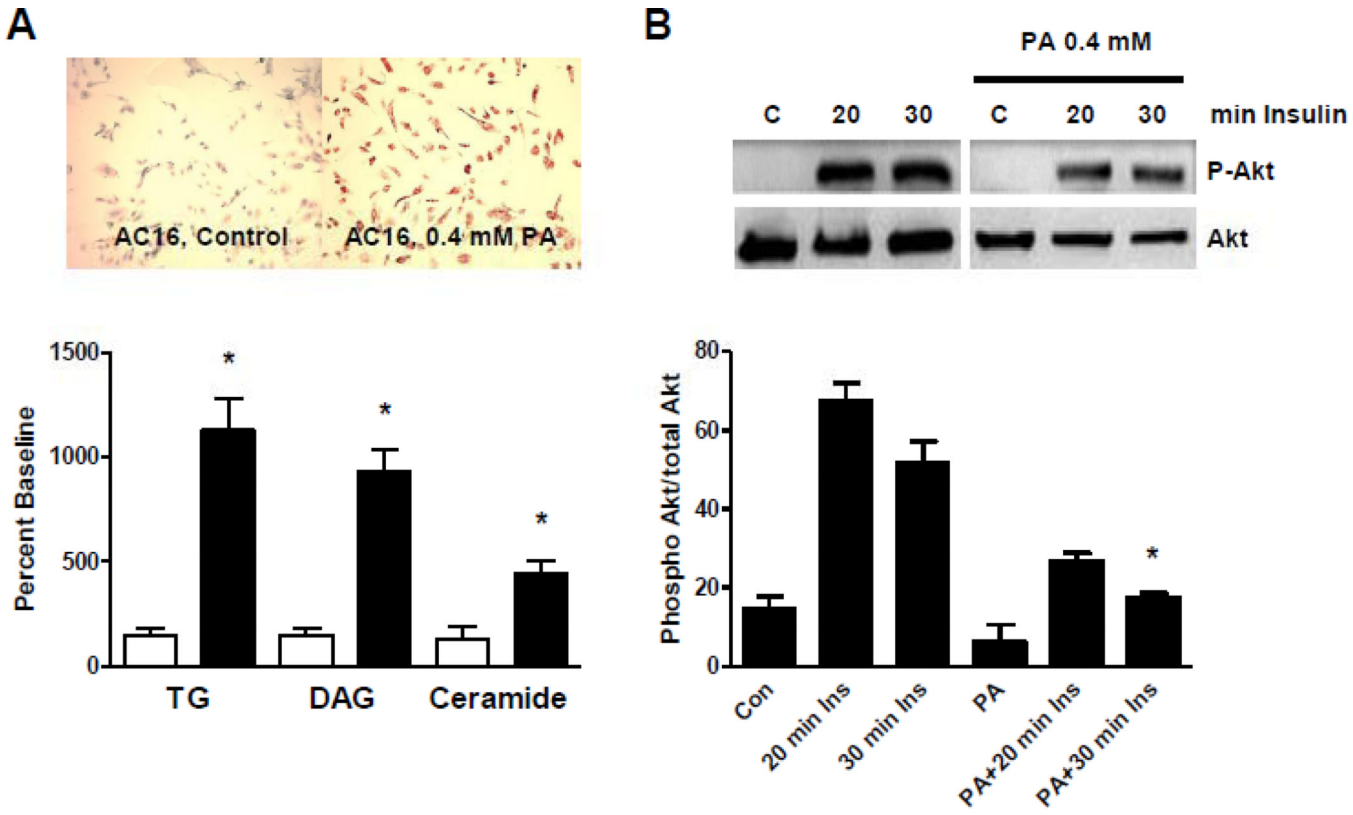

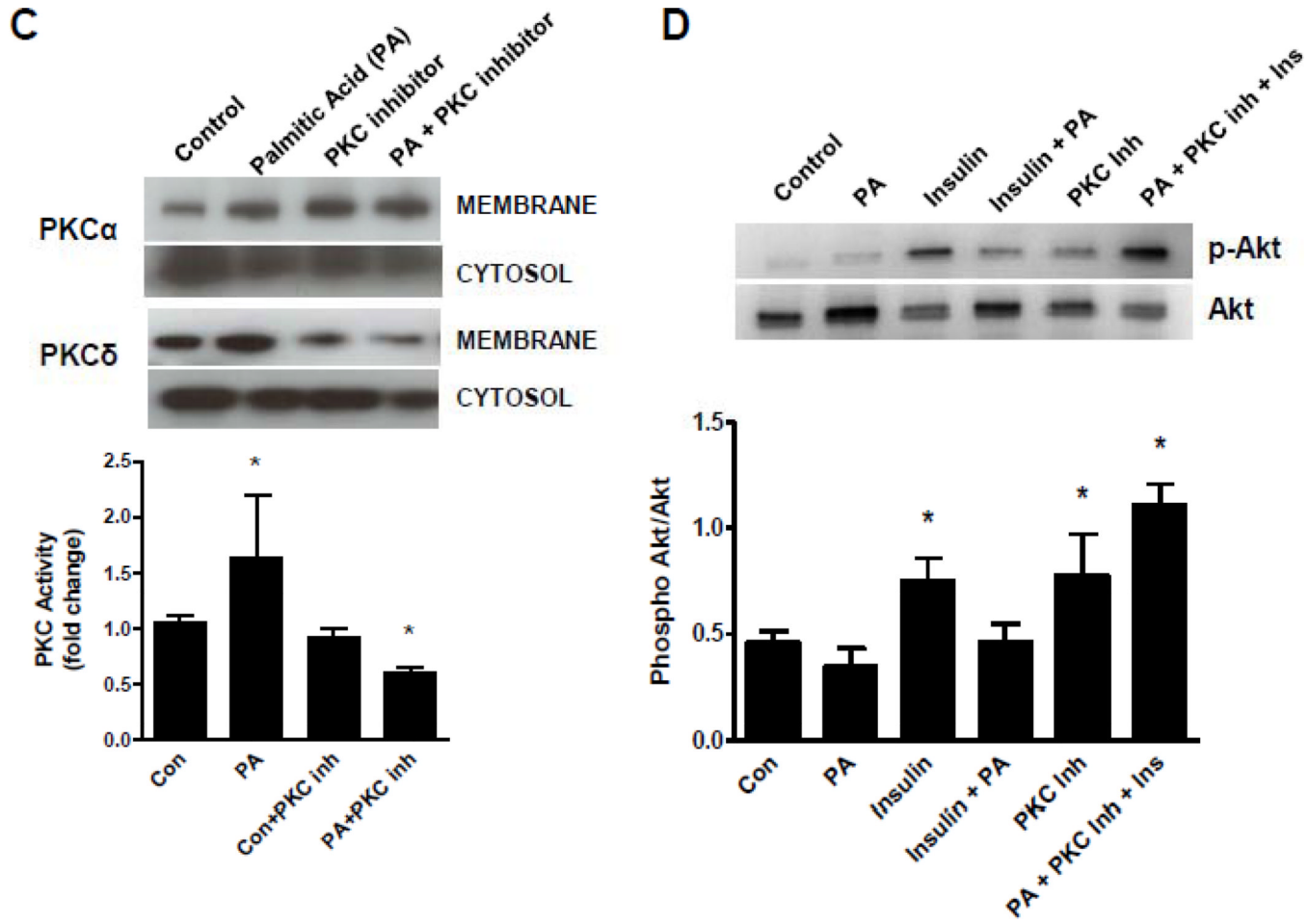

Figure 3.

Inhibition of insulin signaling by increased cardiomyocyte lipid content. (**A**) Incubation of AC16 cells with 0.4 mM palmitic acid (PA) resulted in increased cellular lipid content measured by oil red O staining (top) and by quantitative lipid analysis (bottom, *p<0.05 vs. unstimulated cells). (**B**) Overnight stimulation of AC16 cells resulted in inhibition of insulin-mediated phosphorylation of Akt (*p<0.05 vs. 30 min insulin). (**C**) PKC activity in control and PA-treated cells. (**D**) Inhibition of PKC activity normalized insulin-mediated Akt phosphorylation in AC16 under high PA stimulation (n=3–4 individual samples per group, *p<0.05 vs. control).

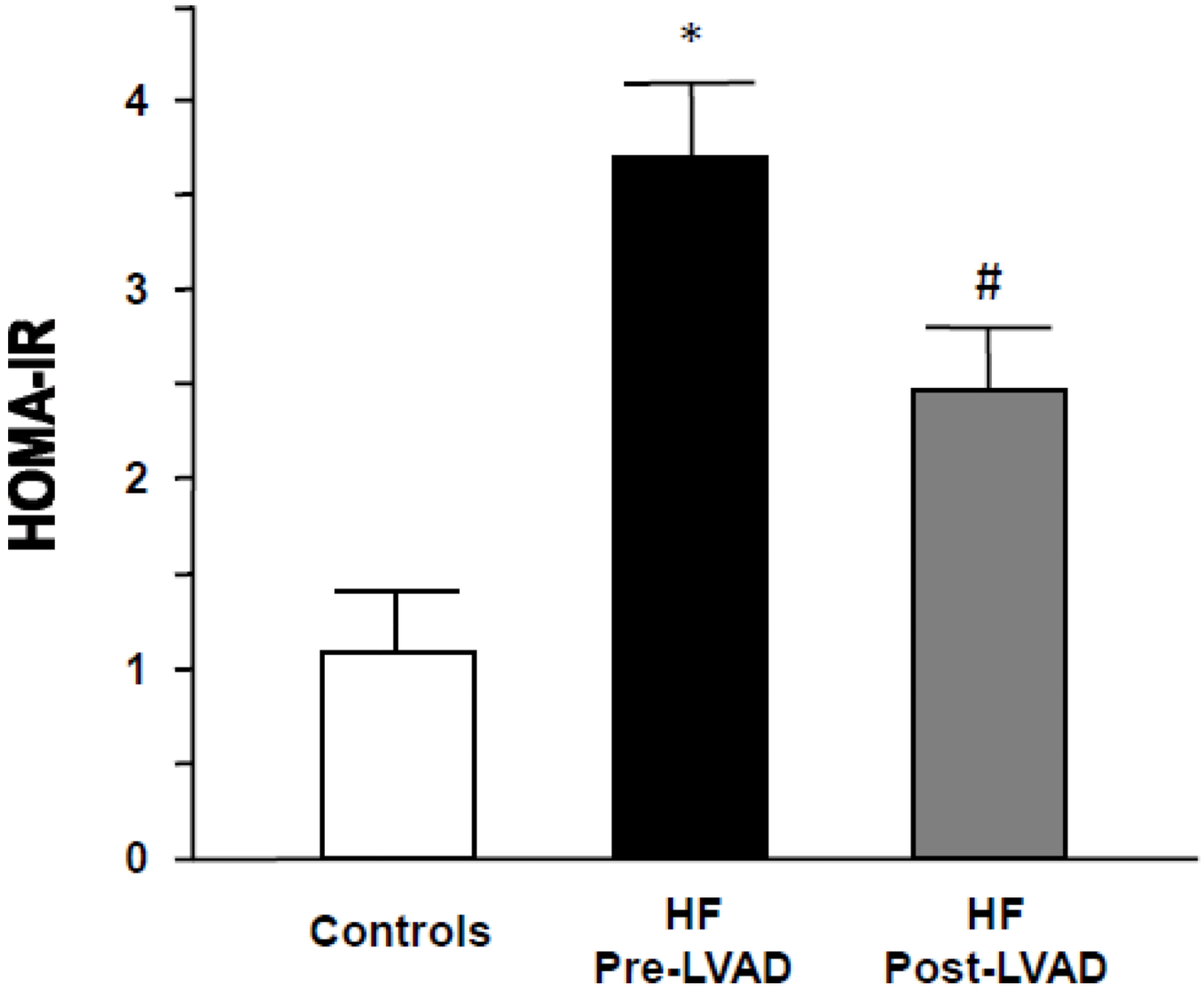

Figure 4.
Insulin resistance in patients with advanced HF corrects following LVAD placement (white bars – controls, n=10; black bars – HF pre-LVAD, n=36; grey bars – HF post-LVAD, n=30; *p<0.01 vs. controls; #p<0.05 vs. HF pre-LVAD).

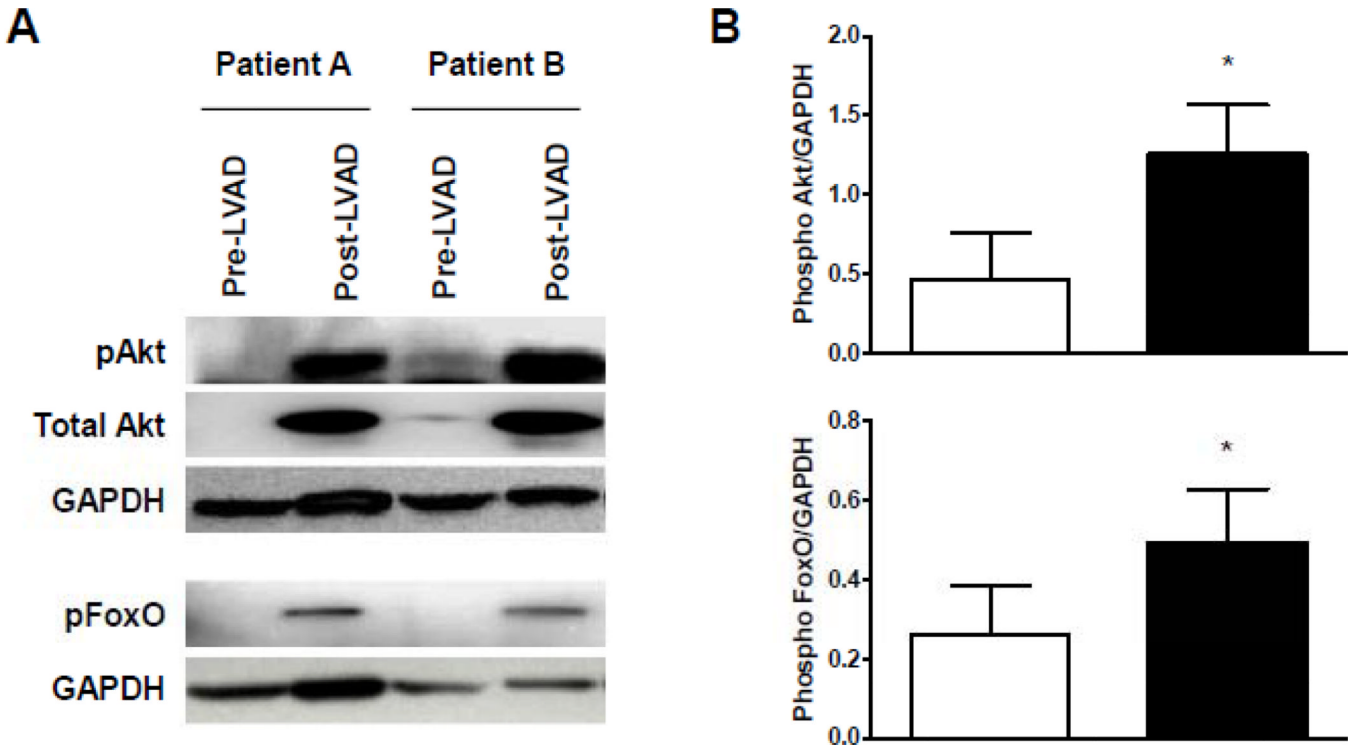

Figure 5.

Mechanical unloading of the failing myocardium increased cardiac PI3K/Akt/Foxo signaling. (**A**) Increased myocardial activation of Akt and Foxo following LVAD placement. (**B**) Quantitative analysis of Akt and Foxo activation. (empty bars – pre-LVAD; filled bars – post-LVAD; n=6 individual patients before and after LVAD implantation; *p<0.05 vs. pre-LVAD).

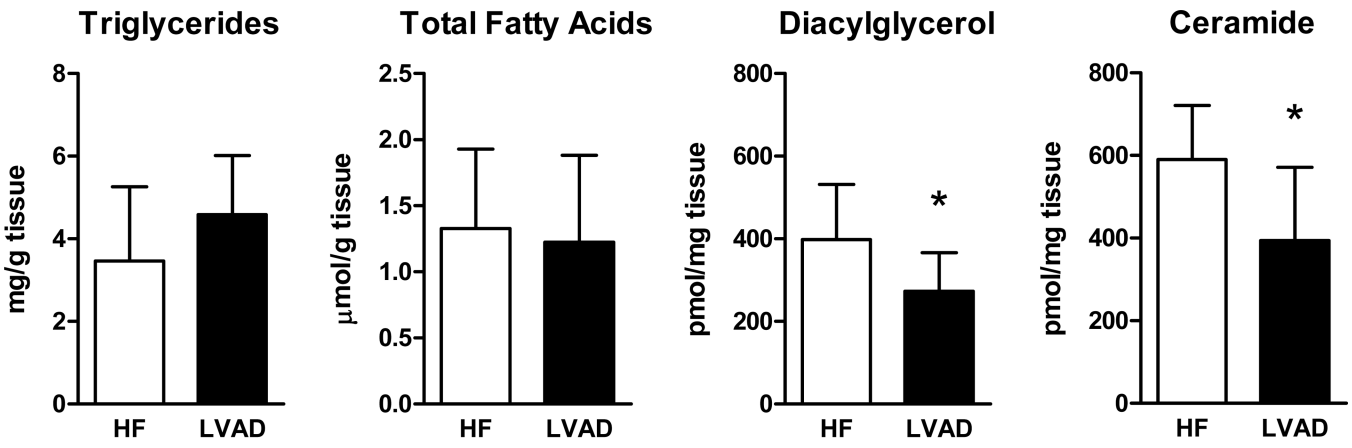

A

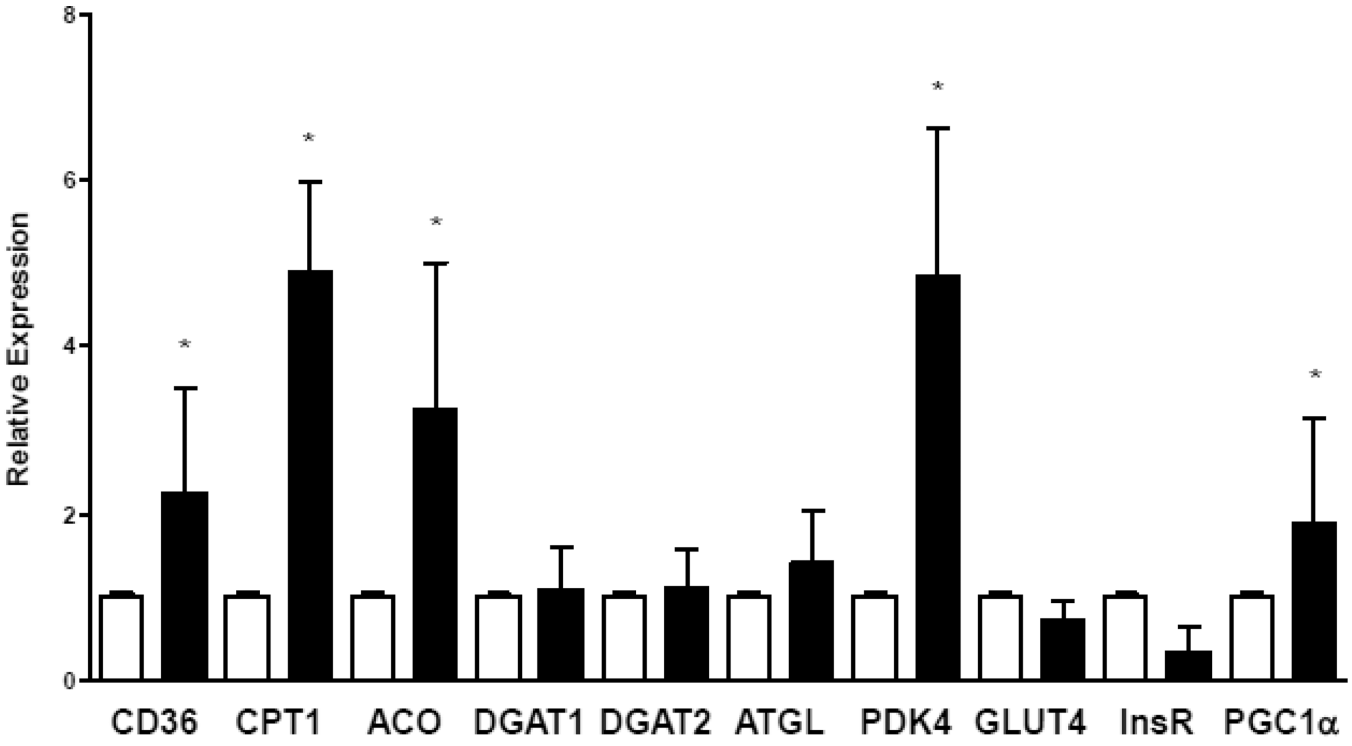

B

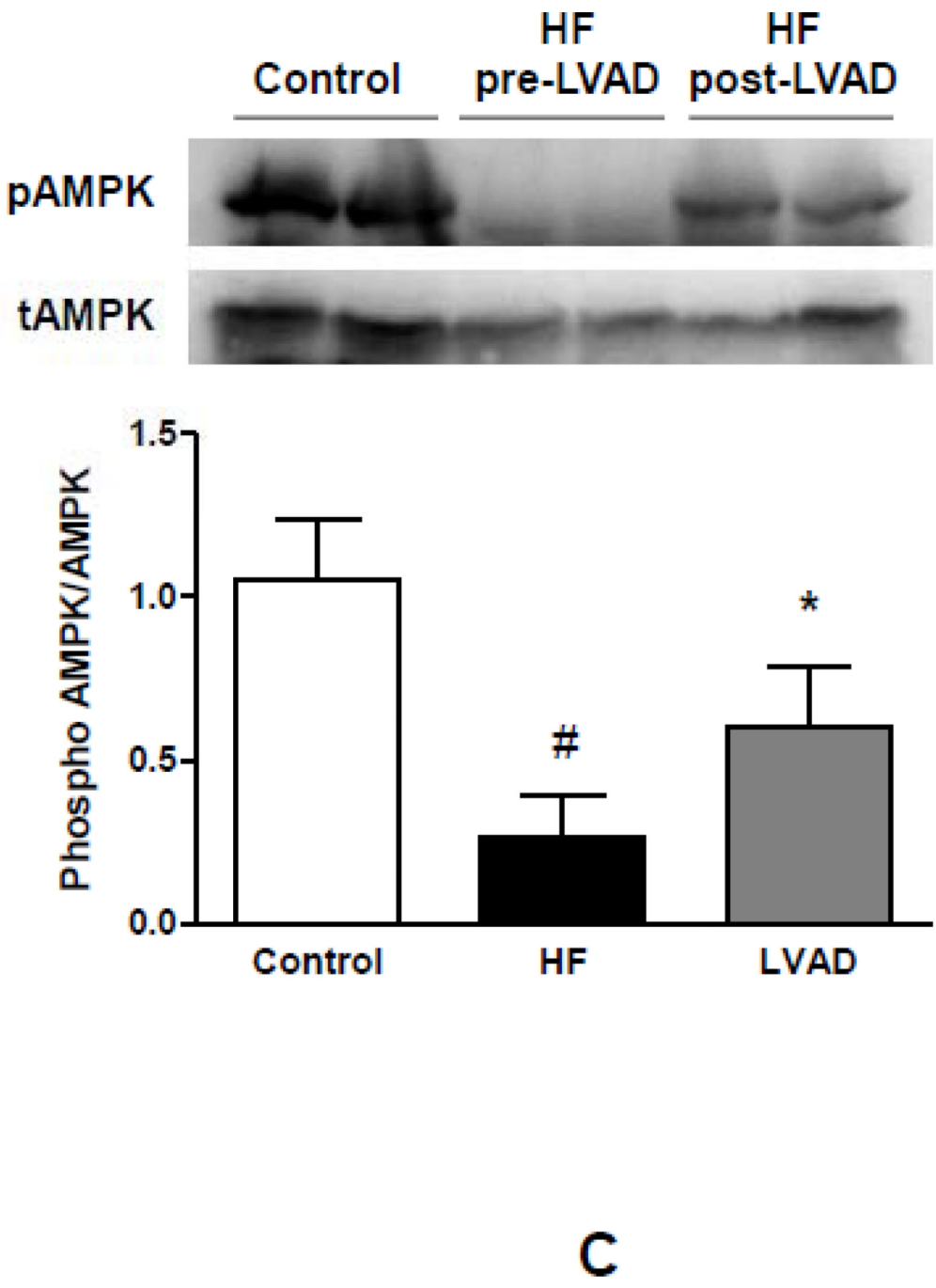

Figure 6.

Impact of mechanical unloading on myocardial lipid content, metabolic gene expression and AMPK activation in patients with advanced HF. (**A**) No changes are detectable in cardiac levels of triglycerides and free fatty acids. Increased levels of DAG and ceramide in advanced HF correct after mechanical unloading of the failing myocardium. (**B**) Changes in myocardial metabolic gene expression in response to mechanical unloading (empty bars – pre-LVAD; filled bars – post-LVAD; *p<0.05 vs. pre-LVAD). (**C**) Reduced myocardial AMPK phosphorylation in patients with advanced HF compared to controls partially corrects after mechanical unloading of the failing myocardium (empty bars – controls; filled

bars - pre-LVAD; grey bars – post-LVAD; *p<0.05 vs. pre-LVAD; #p<0.01 vs. controls; n=6–8 individual patients before and after LVAD implantation).

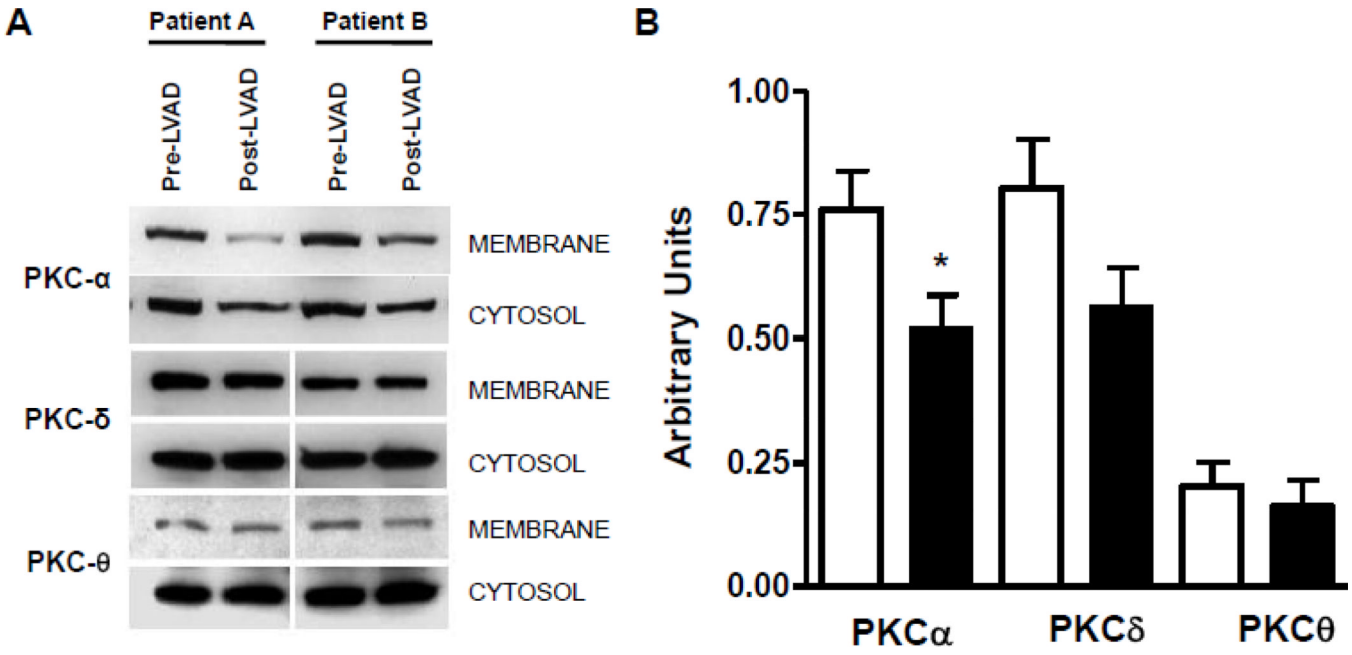

Figure 7.

Myocardial activation of PKC isoforms in patients with advanced HF before and after mechanical unloading. (**A**) Decreased membrane localization of PKC isoforms following mechanical unloading through ventricular assist device placement. (**B**) Semiquantitative assessment of PKC isoform localization (empty bars – pre-LVAD; filled bars – post-LVAD; n=8 individual patients before and after LVAD implantation; *p<0.05 vs. pre-LVAD).

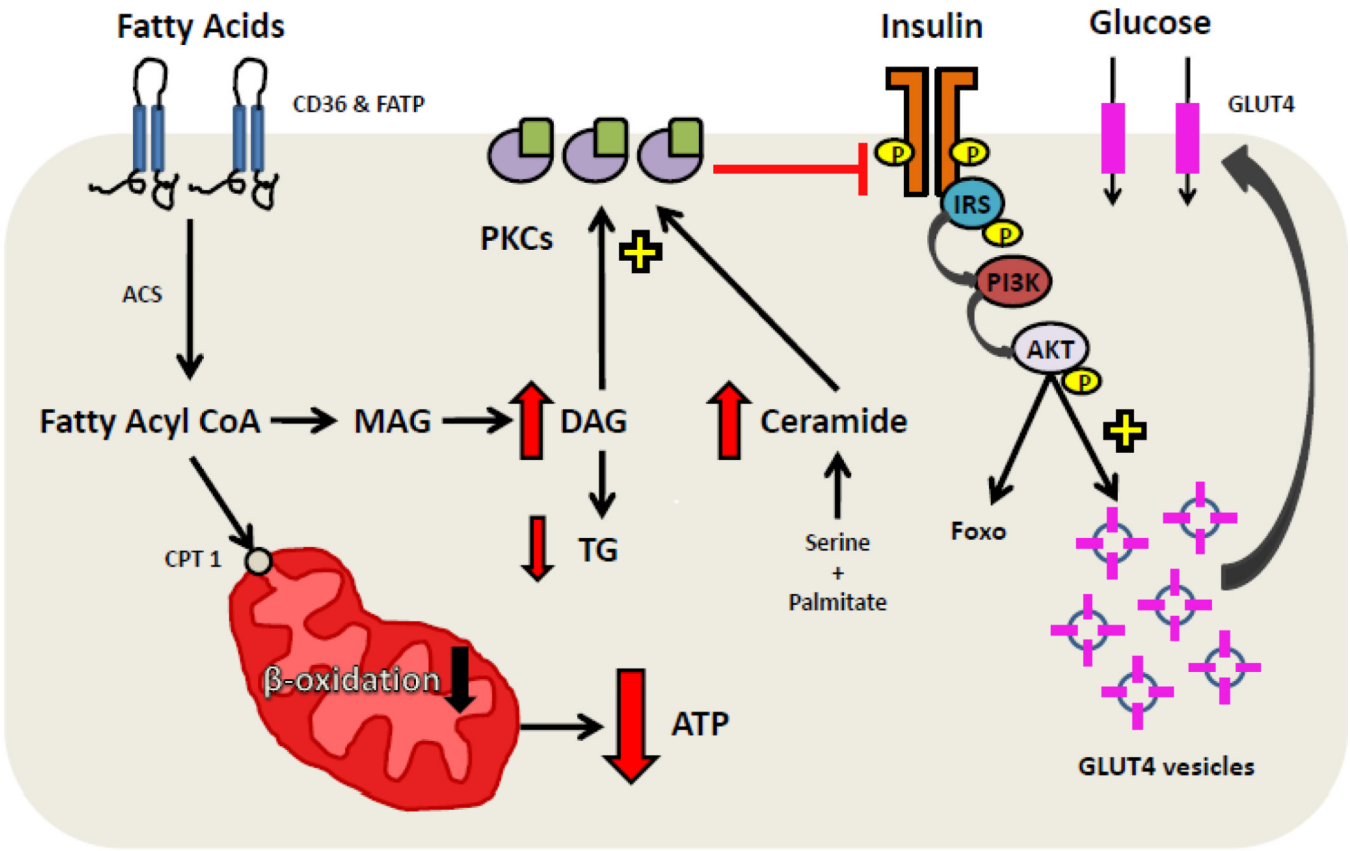

Legend: CD36 – cluster of differentiation 36; FATP – fatty acid transport protein; PKC – protein kinase C; IRS – insulin receptor substrate; PI3K – phosphatidylinositol-3-kinase; GLUT4 – glucose transporter type 4; Foxo – Forkhead transcription factor; DAG – diacylglycerol; TG – triglyceride; MAG – monoacylglycerol; ACS – fatty acid CoA synthetase; CPT1 – carnitine palmitoyltransferase 1

Figure 8.

Lipotoxic inhibition of insulin signaling in advanced HF. CD36 – cluster of differentiation 36; FATP – fatty acid transport protein; PKC – protein kinase C; IRS – insulin receptor substrate; PI3K – phosphatidylinositol-3-kinase; GLUT4 – glucose transporter type 4; Foxo – forkhead transcription factor; GSK3 – glycogen synthase kinase 3; p70s6k – 70-kDa ribosomal protein S6 kinase; DAG – diacylglycerol; TG – triglyceride; MAG – monoacylglycerol; ACS – fatty acid CoA synthase; CPT1 – carnitine palmitoyltransferase 1.

Table 1

Baseline characteristics of patients undergoing LVAD implantation.

Age at Implant, yrs (mean ± SD)	55 ± 13.4
Gender	52 M / 9 F
BMI, kg/m^2 (mean ± SD)	26.5 ± 5.29
<19	5%
19–25	35%
25–30	40%
>30	20%
History of Smoking	51%
Type 2 Diabetes Mellitus	23%
Hypertension	34%
Hyperlipidemia	46%
Etiology of Heart Failure	
Ischemic Cardiomyopathy	59%
Dilated Cardiomyopathy	41%
Ejection Fraction, % (mean ± SD)	18 ± 5.5
LVAD Duration, days (mean ± SD)	177 ± 146

Table 2

Echocardiographic parameters of patients before and after LVAD implantation.

	Pre-VAD	Post-VAD	*p*-value
LVEDD (mm)	69 ± 12	55 ± 15	<0.0001
LVESD (mm)	63 ± 13	48 ± 17	<0.0001
LVEF (%)	17 ± 2	25 ± 15	0.003
IVS (mm)	10 ± 3	11 ± 2	NS
PWT (mm)	10 ± 2	11 ± 2	NS

Table 3

Laboratory parameters before and after LVAD implantation.

	Pre-VAD	Post-VAD	*p*-value
Complete Blood Count			
Hematocrit, %	34.0 ± 5.1	35.0 ± 6.7	NS
Hemoglobin, g/dL	11.1 ± 1.9	11.6 ± 2.2	NS
MCV, fl	88 ± 7.0	88 ± 7.1	NS
Renal Function			
BUN, mg/dL	40 ± 21	27 ± 17	<0.01
Creatinine, mg/dL	1.7 ± 0.8	1.4 ± 0.6	<0.05
Hepatobiliary Function			
AST, U/L	65 ± 127	35 ± 22	0.12
ALT, U/L	67 ± 123	31 ± 247	0.06
Total bilirubin, mg/dL	2.3 ± 5.1	0.8 ± 0.4	0.06
Total protein, g/dL	6.5 ± 1.0	7.4 ± 1.0	<0.001
Albumin, g/dL	3.5 ± 0.6	4.0 ± 0.6	<0.001
Alkaline Phosphatase, U/L	101 ± 61	120 ± 104	NS
Glucose and Lipid Metabolism			
Glucose, mg/dL	137 ± 49	112 ± 41	<0.01
HbA1c, %	7.0 ± 1.6	6.1 ± 1.3	<0.05
Triglycerides, mg/dL	118 ± 69	163 ± 106	<0.05
Cholesterol, mg/dL	129 ± 36	170 ± 50	<0.001
HDL, mg/dL	34 ± 12	48 ± 15	<0.001
LDL, mg/dL	71 ± 27	104 ± 42	<0.001